

# Effects of mixed electric field on characterization of electrohydrodynamics drying system

Amir Abbas Heidari, Pourya Seyfi, Ahmad Khademi, and Hamid Ghomi\*

## Abstract

In this paper, we present a new structure of applying two electrical power supplies to generate ionic wind. In this configuration, two power supplies were applied simultaneously with a modulated voltage to an electrohydrodynamic (EHD) system then corona discharge parameters and EHD thrust characterization was investigated by a corona dryer mechanism. The EHD thrust experiments were performed with a pin to plate and SDBD arrangements. The results show that with the simultaneous application of two power supplies the drying rate in a drop of water as a standard sample was greatly enhanced and the drying time was reduced. Thus, the total evaporation was occurred in 1 minute in the SDBD structure with a power of 7 watts and in 1.5 minutes in pin to plate structure with a power of 2.5 watts. Eventually, it was observed that the use of mixed electric fields enhances the ionic wind, hence increases the non-thermal evaporation process significantly. Furthermore, the drying rate has grown notably in SDBD configuration.

## Keywords

Ionic wind, Modulated voltage, Electrohydrodynamic (EHD), Corona discharge, Surface dielectric barrier discharge (SDBD).

*Laser and Plasma Research Institute, Shahid Beheshti University, Evin 1983963113, Tehran, Iran*

\*Corresponding author: h-gmdashty@sbu.ac.ir

## 1. Introduction

Over the last decade, electro-hydrodynamic (EHD) technology has gained great interest to solve some problems in different industries [1–4]. Cooling and desalination systems based on electrohydrodynamic technology are among the industries that researchers have focused more on in recent years [5–7]. With the increasing advancement in microelectronics, cooling of the micro-sized components has become an important issue in which conventional cooling methods such as water-cooling and air-cooling systems may not be adequate [8–10]. So, due to some limitations in the use of these techniques, as well as high energy consumption and low efficiency, these methods are being replaced with electrohydrodynamic systems over time [11, 12]. Also, considering the importance of fresh-water in the world, desalination systems equipped with an electro-hydrodynamic system are of special importance due to increasing the efficiency of these systems [13]. The electrohydrodynamic effect occurs when high voltage is applied to two asymmetric electrodes, mainly in the form of the pin to plate configuration which the sharp and the plate electrodes act as emitter and collector electrodes respectively [14–16]. The structure of the electrodes and characteristics of the power supplies play a vital role in the discharge, thus any changes in the structure of the electrodes and arrangements of the power supplies will have a significant influence on the desired performance and output efficiency of electrohydrodynamic systems [17–19]. The high intensity of the electric field around the

sharp electrode leads to the ionization of the air in the vicinity of the electrode [20]. The ionized air leads to corona discharge and accumulation of space electric charge [21]. Eventually, this process leads to the propulsion of ionized molecules to the plate electrode, which is known as corona wind or electric wind [22]. The propagation of the corona wind can also be controlled by some special structures, which increases the application and popularity of EHD systems [23, 24]. These structures are based on the surface dielectric barrier discharge (SDBD) called plasma actuators [25–27]. The SDBD structure consists of two electrodes mounted on a dielectric surface with a specific pattern. Corona wind occurs when the strength of the electric field is high enough to ionize the gas followed by plasma discharge. The parameters of corona wind in this structure depend on factors such as electrode pattern, type and thickness of barriers, and applied power supplies [25, 28]. It has been proven that positive high voltage has a higher efficiency in electrohydrodynamic effects compared to negative high voltage [26]. In this paper, we want to investigate the effects of mixed electric fields on the efficiency modifications in the EHD effect by studying the non-thermal evaporation of water droplets in both pin-to-plate and SDBD structures.

## 2. Materials and methods

A scheme of the experimental setup is shown in Figure 1. This schematic is a pin to plate structure. A 5 cm steel needle was used as the pin. The plate used in this structure is made of

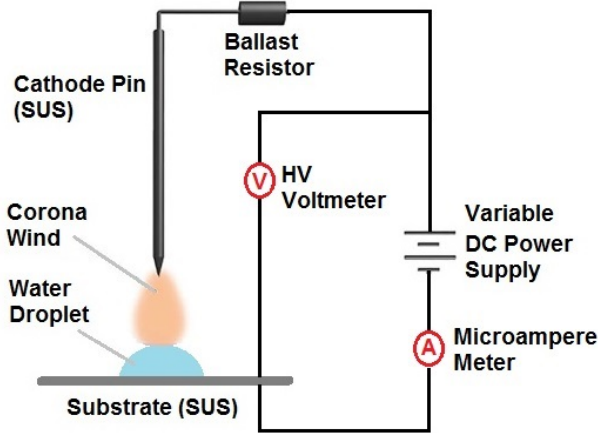


**Figure 1.** The schematic of the experimental Pin to Plate set-up (powered with DC power supply) and measurement tools.

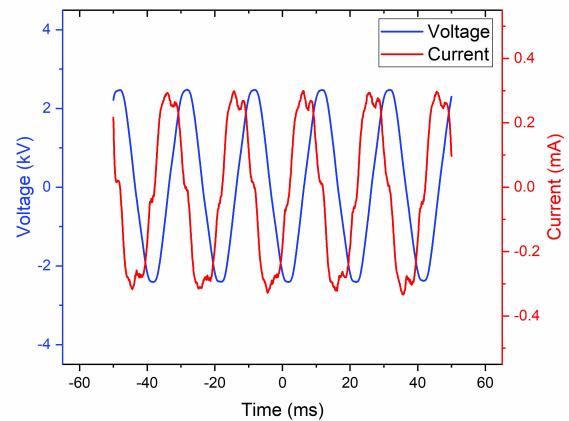


**Figure 4.** The voltage and current waveforms of 50Hz sinusoidal power supply.

metal (stainless steel (SUS;SUS304) ( $30 \times 30 \text{ mm}^2$ )). The

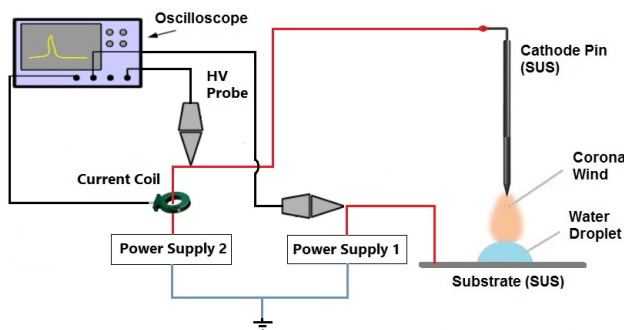


**Figure 2.** The schematic of the experimental Pin to Plate set-up (powered with mixed electric field) and measurement tools.

KV. In the second step, as shown in the schematic in Figure 2, the bias of the structure changes. The two power supplies are used simultaneously as shown in Figure 2. The power source used in the experiments, capable of generating a variable high voltage with sinusoid amplitude at fixed frequency equal to 50 Hz, The corresponding waveform and voltage-current diagram versus time are shown in Figure 4. The other power

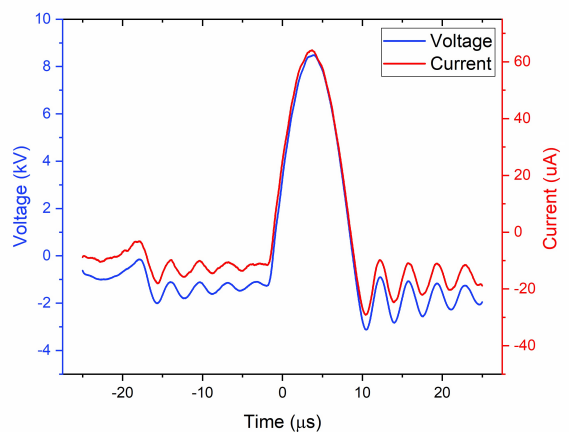


**Figure 5.** The voltage and current waveforms of 6 kHz pulsed power supply.

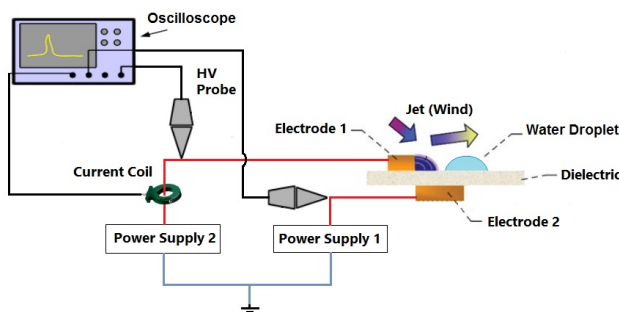


**Figure 3.** The schematic of the experimental SDBD set-up (powered with mixed electric field) and measurement tools.

pin distance to the plate is fixed at two centimeters. In the first step, this structure is biased by a direct current power supply. The output voltage of this source varies from 0 to 30

source , capable of generating a variable amplitude of pulsed high voltage at 6 kHz frequency, the corresponding waveform and voltage-current diagram versus time are shown in Figure 5. In the last step, the surface dielectric barrier discharge (S-DBD) structure is used as shown in the schematic in Figure 3. The two electrodes are mounted exactly tangentially on the surface. The electrodes are selected from a 1 mm thick copper foil (electrode1 ( $10 \times 10 \text{ mm}^2$ ) and electrode2 ( $10 \times 20 \text{ mm}^2$ )). The dielectric of the glass is also selected with a thickness

of 2 mm (30×30 mm<sup>2</sup>). The temperature distribution on the substrate surface was measured by Fluke VT04A Visual IR Thermometer. The voltage and the current are measured by a high voltage probe (TEKTRONIX P6015 1:1000) and a current probe (TCP202 TEKTRONIX), respectively. The electrical signals are visualized using a TEKTRONIX TDS 2024B oscilloscope (200 MHz). The following equations are used to calculate the average electrical power applied to the plasma jet. Where  $P_{ave}$  and  $P(t)$  are the average and time-dependent electrical power, respectively,  $E_{pulse}$  is the energy per pulse,  $V(t)$  and  $I(t)$  are the time-dependent voltage and current, respectively.

$$P(t) = V(t) \times I(t) \tag{1}$$

$$E_{pulse} = \int_0^T P(t)dt \tag{2}$$

$$P_{ave} = \frac{E_{pulse}}{T} \tag{3}$$

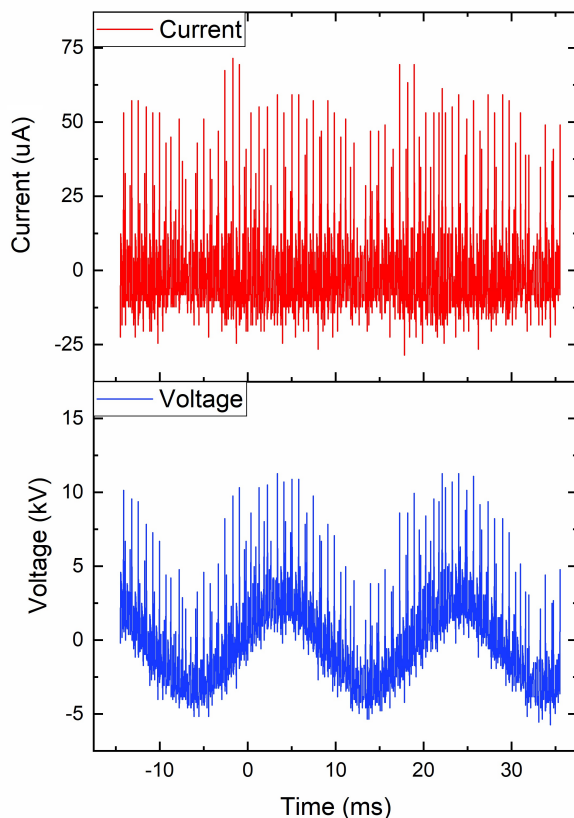


**Figure 6.** The voltage and current waveforms when both power supplies are applied simultaneously (Amplitude-Modulated power supply).

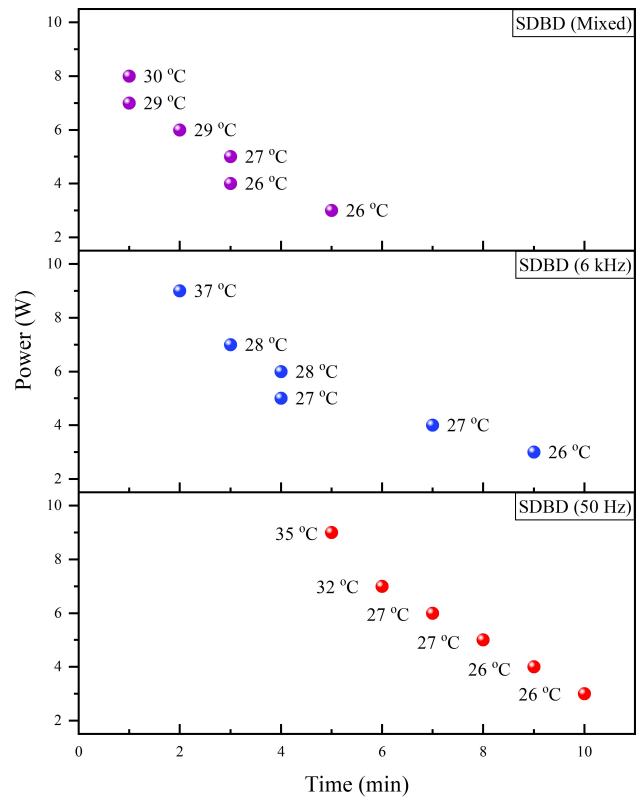


**Figure 7.** Maximum treatment time in electrical power variations (SDBD structure).

$$P_{TOTAL} = P_{ave}(6KHz) + P_{ave}(50Hz) \tag{4}$$

The total power consumption of two power supplies is shown by  $P_{TOTAL}$ . The volume of water droplet was 10 microliter. The ionic wind velocity was also measured by the structure of the pitot tube exactly at the point of the water droplet.

### 3. Results and discussion

As shown in Figure 6, the electric field of the modulated power supply generates plasma. The behavior of the modulated electric field (Amplitude Modulation) as well as the effects of the electric fields of the carrier wave and the electric field carried in the amplitude are investigated separately. Figure 7 shows the studies performed for the structure of a SDBD. The same studies have been performed for Pin to Plate structure and are reported in Figure 8. As can be seen, the applied electrical power is directly related to the drying time of the drop. The duration decreases linearly with increasing power. But with this increase we reach a point where with increasing electrical power the surface temperature increases non-linearly. This increase in temperature is observed in all existing structures, so the criterion for comparison is a non-linear variation in temperature. In the SDBD structure, it is observed that the drying rate of the droplet is accelerated by increasing the frequency.

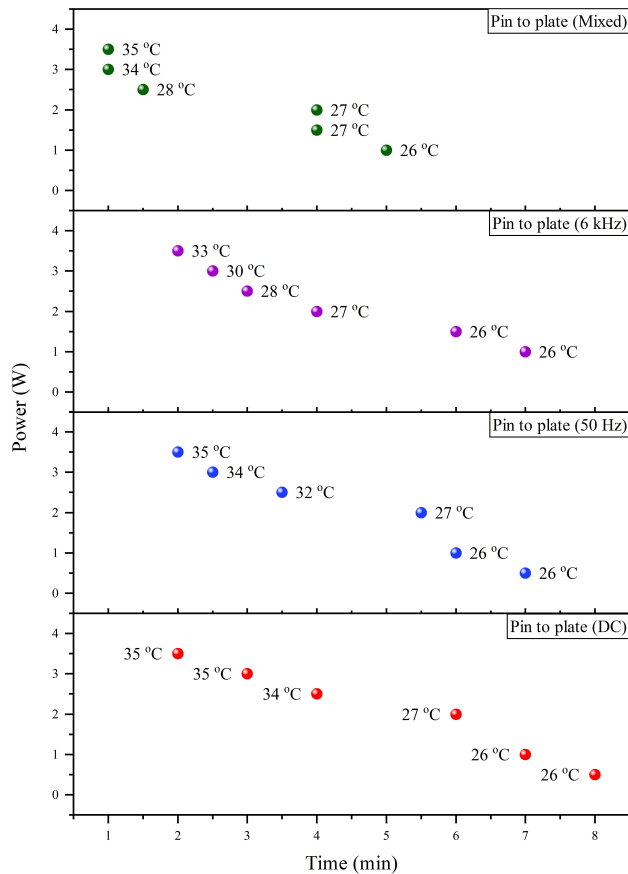


**Figure 8.** Maximum treatment time in electrical power variations (Pin to Plate structure).

In the final step, it was observed that using a mixed electric field, both the ionic wind speed at the surface increased towards the droplet and we had a lower surface temperature at equal power than other structures. This behavior can be due to the control of the charge on the surface and the control of the behavior of the plasma by the voltage modulated. It has been proven that ion winds move parallel to the surface and increase its velocity. On the other hand, in the Pin to Plate structure, the ionic wind movement and its velocity changes in the direction perpendicular to the surface. Carefully in the results of the Pin to Plate structure it is observed that the reinforcement process at the time of drying is almost the same compared to the SDBD structure. The final comparison diagram of the drying time in different power supply structures in the two main configurations is reported in Figure 9. Comparison of the final results clearly shows the enhancing of the dryer performance in the structure of the mixed electric field. In temperature studies, it is clear that amplification effects are not related to temperature effects. For a more detailed study ionic wind velocities were measured in all conditions and are reported in Figure 10. This measurement was performed according to the conditions of Figure 9. The trend of ion wind velocity increase is shown in the diagram. Finally, the effects of amplification in the drying process can be attributed to the

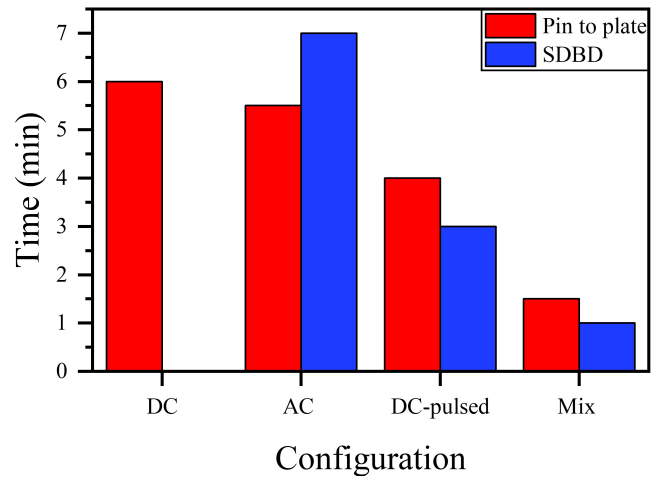


**Figure 9.** Final comparison of dryer time in the structure of different power supplies in two main configurations.

combination of mixed electric field behaviors in increasing the ionic wind speed.

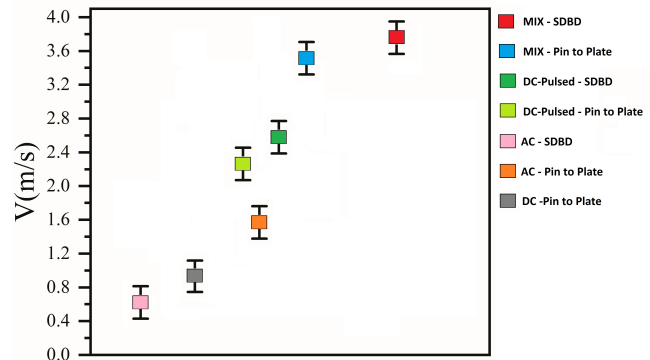


**Figure 10.** Diagram of ion wind velocity variations in all structures studied.

### 4. Conclusion

An experimental study of EHD drift generated in pin to plate and SDBD arrangements was performed by applying mixed electric fields and its performance was compared with conventional power supplies. The performance of EHD drift in this study has been investigated by non-thermal evaporation of water droplets. In this experiment, by changing the applied power to the system in the mixed electric field, the efficiency of the non-thermal evaporation of water was investigated. The applied power was changed in such a manner that, the minimum time for total evaporation of the water droplet was achieved at a controlled temperature. Experimental results showed a linear relationship between EHD drift, applied power, and evaporation rate of the water droplet. Thus, as the applied power increases, the evaporation rate of water droplet also increases, but the increase in the power should not be as

much to lead to a change in the plasma regime and an increase in water temperature and this can be seen in the mixed electric field in both structures. To prove this process by measuring ionic wind velocity, the linear relationship of ionic wind velocity increase in a mixed electric field with enhance drying effects was also clearly seen.

#### Conflict of interest statement:

The authors declare that they have no conflict of interest.

## References

- [1] F.C. Lai. *Journal of Electrostatics*, **106**:103469, 2020.
- [2] J. Wang, R. Fu, and X. Hu. *Journal of Electrostatics*, **100**:103358, 2019.
- [3] C.P. Tien, S.C. Lin, and F.C. Lai. *Journal of Electrostatics*, **107**:103482, 2020.
- [4] A. Mushyam, F. Rodrigues, and J. C. Pascoa. *International Journal for Numerical Methods in Fluids*, **90**:115, 2019.
- [5] A. Yabe, Y. Mori, and K. Hijikata. *AIAA journal*, **16**:340, 1978.
- [6] Y.J.Chang, J.C. Peng, S.C. Lin, and F.C. Lai. *Journal of Electrostatics*, **105**:103438, 2020.
- [7] J. Wang, T. Zhu, J. Wang, Y. Cai, and X. Li. *Sustainable Energy Technologies and Assessments*, **39**:100703, 2020.
- [8] M. Cogollo, P. M. Balsalobre, A. Díaz Lantada, and H. Puago. *Applied Sciences*, **10**:1010, 2020.
- [9] J. Wang, T. Zhu, Y. Cai, J. Zhang, and J. Wang. *International Journal of Heat and Mass Transfer*, **152**:119545, 2020.
- [10] J. Wang, T. Zhu, Y. Cai, J. Wang, and J. Wang. *Applied Thermal Engineering*, **169**:114922, 2020.
- [11] S. Sato, H. Furukawa, A. Komuro, M. Takahashi, and N. Ohnishi. *Scientific reports*, **9**:1, 2019.
- [12] M.D. Babushkin, A. V. Kashin, and K. G. Antipova. *Journal of Physics: Conference Series*, **1393**:012073, 2019.
- [13] V.K. Patel and J. Seyed-Yagoobi. *IEEE Transactions on Industry Applications*, **50**:3011, 2014.
- [14] Q.K. He, H. Liang, and B.R. Zheng. *Chinese Physics B*, **29**:064702, 2020.
- [15] A. Krupa, J. Podliński, J. Mizeraczyk, and A. Jaworek. *Powder Technology*, **344**:475, 2019.
- [16] J. Wang, R. Fu, and X. Hu. *Applied Thermal Engineering*, **148**:457, 2019.
- [17] A. K. M. M. H. Mazumder and F.C. Lai. *Journal of Electrostatics*, **99**:49, 2019.
- [18] M.G.De. Giorgi, V. Motta, and A. Suma. *Aerospace Science and Technology*, **96**:105587, 2020.
- [19] Z. YE, J. ZOU, and Y. ZHENG. *DEStech Transactions on Computer Science and Engineering icaic*, , 2019.
- [20] S.A. Vasilkov, K. D. Poluektova, and Y.K. Stishkov. *Physics of Fluids*, **32**:107102, 2020.
- [21] J. Little, A. Singh, T. Ashcraft, and C. Durasiewicz. *Plasma Sources Science and Technology*, **28**:014002, 2019.
- [22] J.W. Lee, D.K. Sohn, and H.S. Ko. *Journal of Mechanical Science and Technology*, **34**:3679, 2020.
- [23] M. Bouadi, K. Yanallah, M. R. Bouazza, and F. Pontiga. *ICREEC 2019, 2020 - Springer*, :465, 2020.
- [24] A. Martynenko, T. Astatkie, and T. Defraeye. *Journal of Food Engineering*, **271**:109777, 2020.
- [25] Y. Long, H. Li, X. Meng, J. Li, and Z. Xiang. *Modern Physics Letters B*, **32**:1850315, 2018.
- [26] Z. Zilu, Y. Dezheng, W. Wenchun, Y. Hao, L. Zhang, and S. WANG. *Plasma Science and Technology*, **19**:064007, 2017.
- [27] A. Devarajan. *pstorage-purdue-258596361474*, , 2019.
- [28] J. Li, L.I. Xiuqian, Z. Zhang, X. Che, W. Nie, and Z. Zheng. *Advances in Materials, Machinery, Electrical Engineering (AMMEE)*, **114**:578, 2017.